Hourglass charge-three Weyl phonons

Xiaotian Wang,[1,*,†] Feng Zhou,[1,*] Zeying Zhang,[2,3] Zhi-Ming Yu,[4,5,‡] and Yugui Yao[4,5]

[1]*School of Physical Science and Technology, Southwest University, Chongqing 400715, China*

[2]*College of Mathematics and Physics, Beijing University of Chemical Technology, Beijing 100029, China*

[3]*Research Laboratory for Quantum Materials, Singapore University of Technology and Design, Singapore 487372, Singapore*

[4]*Centre for Quantum Physics, Key Laboratory of Advanced Optoelectronic Quantum Architecture and Measurement (MOE), School of Physics, Beijing Institute of Technology, Beijing 100081, China*

[5]*Beijing Key Laboratory of Nanophotonics & Ultrafine Optoelectronic Systems, School of Physics, Beijing Institute of Technology, Beijing 100081, China*

(Received 21 September 2022; revised 15 November 2022; accepted 8 December 2022; published 19 December 2022)

The unconventional Weyl point with nonlinear dispersion features higher topological charge $|\mathcal{C}| > 1$ and multiple topologically protected Fermi arc states at its boundary. As a novel topological state, it has been attracting widespread attention. However, the unconventional Weyl point with $|\mathcal{C}| = 3$ has not yet been reported in realistic materials, even though it has been theoretically proposed for more than a decade. In this work, based on first-principles calculations and theoretical analysis, we predict the existing material α-$LiIO_3$ as the first realistic example with this unconventional Weyl point. Specifically, in the phonon spectra of α-$LiIO_3$, two Weyl points with $\mathcal{C} = -3$, connected by time-reversal symmetry, appear at the neck crossing point of an hourglass-type band, leading to two hourglass charge-3 Weyl phonons. The symmetry protection and the associated novel triple- and sextuple-helicoid surface arc states of the hourglass charge-3 Weyl phonons are revealed. Our results uncover a hidden topological character of α-$LiIO_3$ and also show that the phonon spectra are a great platform for exploring unconventional topological states.

DOI: 10.1103/PhysRevB.106.214309

I. INTRODUCTION

In the past decades, one of the most important findings in condensed matter physics is the prediction of the topological Weyl semimetal [1,2], which shows that elementary particles such as the Weyl fermion can emerge as low-energy excitations in topological semimetal materials, opening the door for simulating interesting phenomena in astrophysics and general relativity on laboratory tables [3]. The conventional Weyl point (WP) exhibits relativistic linear dispersion along any direction in momentum space and carries unit topological charge (Chern number) $|\mathcal{C}| = 1$ [1]. Particularly, it is topologically protected and can exist in three-dimensional (3D) crystals without any space group symmetry (except translation symmetry). Many realistic materials have been predicted as topological Weyl semimetals with conventional WP [4–16], and some of them have been experimentally confirmed [17–21].

In 2012, Fang *et al.* [23] demonstrated that with rotation symmetry, two (three) conventional WPs can merge together, leading to unconventional WP, which exhibits higher topological charge $|\mathcal{C}| = 2$ ($|\mathcal{C}| = 3$) and quadratic (cubic) dispersion in the plane normal to the rotation axis. This pioneering work led to a series of subsequent studies, such as the prediction of the corresponding material candidates [24–31], the demonstration of the novel phenomena of these unconventional WPs [32–36], and the search for other types of unconventional emergent particles [37–41]. Recently, one other species of the unconventional WP, exhibiting topological charge $|\mathcal{C}| = 4$, has been predicted in spinless nonmagnetic systems [42–45] and spinful magnetic systems [46]. The WP with topological charge $|\mathcal{C}| = n$ ($n = 1, 2, 3, 4$) also is termed as the charge-n (C-n) WP [42].

However, up to now, only a few materials were predicted to host the unconventional WPs. Particularly, the C-3 WP has not yet been reported in realistic material. In the beginning, the topological Weyl semimetals were predicted in the materials with strong spin-orbit coupling (SOC) [1,4,47,48]. Later, it was shown that spinless systems also can host WPs due to the pseudo-SOC effect [42], which significantly expands the material candidates database of topological Weyl states. Recently, the search for WPs has shifted toward the phonon spectra of crystals [49–56]. In contrast to the electronic bands, all the phonon bands are relevant for experimental detection, as the phonons are free of the constraint of the Pauli exclusion principle and Fermi surface. Additionally, the topological phonons may lead to novel phenomena in heat transfer, phonon scattering, and electron-phonon interaction [57–60].

In this work, based on theoretical analysis and first-principles calculations, we predict the existing material α-$LiIO_3$ as the first realistic example hosting the C-3 WPs in its phonon spectra. We first show that for spinless systems (such as phonon spectra) with time-reversal symmetry $\mathcal{T}$, the

*These authors contributed equally to this work.

†xiaotianwang@swu.edu.cn

‡zhiming_yu@bit.edu.cn

TABLE I. The candidate SGs that can host (hourglass and normal) C-3 WP in spinless systems. "Irreps" denotes the irreducible (co-)representation of the little group associated with the (hourglass and normal) C-3 WP. The symbols of the irreps are adopted from Ref. [22].

SG No.	SG symbol	Generators	Location	Irreps	Species
168	P6	$\{C_{6z}\|000\}, \mathcal{T}$	Γ-A path	$\{R_1, R_4\}, \{R_2, R_5\}, \{R_3, R_6\}$	Normal C-3 WP
169	$P6_1$	$\{C_{6z}\|00\frac{1}{6}\}, \mathcal{T}$	Γ-A path	$\{R_1, R_4\}, \{R_2, R_5\}, \{R_3, R_6\}$	Normal C-3 WP
170	$P6_5$	$\{C_{6z}\|00\frac{5}{6}\}, \mathcal{T}$	Γ-A path	$\{R_1, R_4\}, \{R_2, R_5\}, \{R_3, R_6\}$	Normal C-3 WP
171	$P6_2$	$\{C_{6z}\|00\frac{1}{3}\}, \mathcal{T}$	Γ-A path	$\{R_1, R_4\}, \{R_2, R_5\}, \{R_3, R_6\}$	Normal C-3 WP
172	$P6_4$	$\{C_{6z}\|00\frac{2}{3}\}, \mathcal{T}$	Γ-A path	$\{R_1, R_4\}, \{R_2, R_5\}, \{R_3, R_6\}$	Normal C-3 WP
173	$P6_3$	$\{C_{6z}\|00\frac{1}{2}\}, \mathcal{T}$	Γ-A path	$\{R_3, R_6\}$	Normal C-3 WP
				$\{R_1, R_4\}, \{R_2, R_5\}$	Hourglass C-3 WP
177	P622	$\{C_{6z}\|000\}, \{C'_{21}\|000\}, \mathcal{T}$	Γ-A path	$\{R_1, R_4\}, \{R_2, R_5\}, \{R_3, R_6\}$	Normal C-3 WP
178	$P6_122$	$\{C_{6z}\|00\frac{1}{6}\}, \{C'_{21}\|000\}, \mathcal{T}$	Γ-A path	$\{R_1, R_4\}, \{R_2, R_5\}, \{R_3, R_6\}$	Normal C-3 WP
179	$P6_522$	$\{C_{6z}\|00\frac{5}{6}\}, \{C'_{21}\|000\}, \mathcal{T}$	Γ-A path	$\{R_1, R_4\}, \{R_2, R_5\}, \{R_3, R_6\}$	Normal C-3 WP
180	$P6_222$	$\{C_{6z}\|00\frac{1}{3}\}, \{C'_{21}\|000\}, \mathcal{T}$	Γ-A path	$\{R_1, R_4\}, \{R_2, R_5\}, \{R_3, R_6\}$	Normal C-3 WP
181	$P6_422$	$\{C_{6z}\|00\frac{2}{3}\}, \{C'_{21}\|000\}, \mathcal{T}$	Γ-A path	$\{R_1, R_4\}, \{R_2, R_5\}, \{R_3, R_6\}$	Normal C-3 WP
182	$P6_322$	$\{C_{6z}\|00\frac{1}{2}\}, \{C'_{21}\|000\}, \mathcal{T}$	Γ-A path	$\{R_3, R_6\}$,	Normal C-3 WP
				$\{R_1, R_4\}, \{R_2, R_5\}$	Hourglass C-3 WP

C-3 WP only appears at the sixfold rotation axis belonging to chiral space groups (SGs). Hence, this unconventional WP can be realized in 12 of the 230 SGs, as listed in Table I. Moreover, the C-3 WP can be further divided into two categories: normal C-3 WP and hourglass C-3 WP, which respectively appear in the SGs without and with sixfold screw rotation symmetry $\{C_{6z}|00\frac{1}{2}\}$. This means that the hourglass C-3 WP only appears in SGs 173 and 182. Guided by the symmetry analysis, we identify the existence of the hourglass C-3 Weyl phonons in several realistic material candidates, including α-$LiIO_3$. More material candidates can be found in the Supplemental Material (SM) [61]. Remarkably, the hourglass-type band and the hourglass C-3 WPs in α-$LiIO_3$ are well separated from other phonon bands. Furthermore, we find that due to the presence of $\mathcal{T}$ symmetry, the hourglass C-3 WPs must come in pairs with the same chirality, leading to a novel sextuple-helicoid surface arc state on the boundary normal to the sixfold screw rotation axis. Our results not only predict the first material candidate hosting C-3 Weyl phonons, but also show that the phonon spectra are a great platform for exploring unconventional topological states.

II. HOURGLASS C-3 WP

As shown in previous works [23,42], for spinless systems with time-reversal symmetry $\mathcal{T}$, the C-3 WP only occurs on the sixfold rotation axis of chiral SGs. Moreover, it cannot reside at the time-reversal-invariant momentum, as the topological charge of the WP at such momentum must be even [62]. Hence, the C-3 WP should be a crossing that appears on the Γ-A high-symmetry path and is formed by two bands with different eigenvalues of the sixfold rotation operator.

Consider a 3D system with $\mathcal{T}$ and sixfold rotation symmetry along the z direction $\tilde{C}_{6z,n} = \{C_{6z}|00\frac{n}{6}\}$ $(n = 0, 1, \ldots, 5)$; then the Bloch states on the axis can be chosen as the eigenstates of $\widetilde{C}_{6z,n}$, denoted as $|(m, n)\rangle$, for which the eigenvalue of $\widetilde{C}_{6z,n}$ is $e^{i2m\pi/6}e^{ik_z n/6}$ $(m = 0, 1, \ldots, 5)$. While each pair of the bands with different (m, n) can cross and form a WP, the C-3 WP is only formed by the two bands with $|(m, n)\rangle$ and $|(m + 3 \bmod 6, n)\rangle$ [23], as the ratio of their eigenvalue of $\widetilde{C}_{6z,n}$ is -1.

Since $\mathcal{T}^2 = 1$, at the Γ (000) and A (00π) points, the state $|(m, n)\rangle$ and its time-reversal partner $\mathcal{T}|(m, n)\rangle = |(-m, -n)\rangle$ will be linearly independent when $e^{i2m\pi/6}e^{ik_z n/6} \neq e^{-i2m\pi/6}e^{-ik_z n/6}$, and must be degenerate at the same energy. Interestingly, for $n = 3$, i.e., $\tilde{C}_{6z,3} = \{C_{6z}|00\frac{1}{2}\}$, the two states $|(1, 3)\rangle$ and $|(5, 3)\rangle$ [$|(2, 3)\rangle$ and $|(4, 3)\rangle$] are degenerate at Γ point, while $|(1, 3)\rangle$ and $|(2, 3)\rangle$ [$|(4, 3)\rangle$ and $|(5, 3)\rangle$] are degenerate at the A point, leading to an hourglass-type band dispersion, as illustrated in Fig. 1. Particularly, the neck crossing point of the hourglass is formed by the states either $|(2, 3)\rangle$ and $|(5, 3)\rangle$ [see Fig. 1(a)] or $|(1, 3)\rangle$ and $|(4, 3)\rangle$ [see Fig. 1(b)], indicating that the neck crossing point here must be a C-3 WP. We term such crossing point as the hourglass C-3 WP. Since only two chiral SGs (SG 173 and SG 182) exhibit $\{C_{6z}|00\frac{1}{2}\}$ (see Table I), the hourglass C-3 WP would be very rare.

Before closing this section, we would like to point out that since proposed in the large-gap insulators KHgX (X = As, Sb, Bi) [63], the hourglass Weyl fermion has attracted widespread interest, as the neck crossing point of an hourglass-type band is a new kind of essential degeneracy that cannot be directly inferred from the irreducible co-representations of the corresponding little group [64]. Subsequently, many counterparts

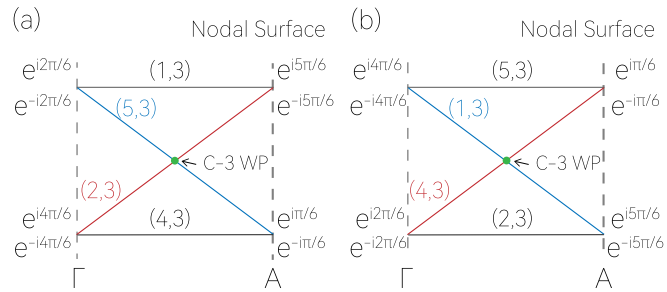

FIG. 1. Formation mechanism of hourglass C-3 WP in spinless systems. (a) and (b) show two possible modes of the hourglass-type bands along Γ-A path.

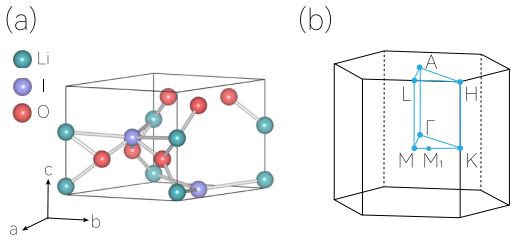

FIG. 2. (a) Crystal structure of α-$LiIO_3$. (b) Bulk BZ of α-$LiIO_3$.

with hourglass-like band topology, such as the hourglass Dirac chain [65,66], hourglass Dirac loop [67], and hourglass Weyl loops [68], are proposed in theory and some of them have been experimentally confirmed. In this work, we report a new kind of hourglass quasiparticle: hourglass C-3 WPs in spinless systems. Our work can be viewed as a guide for further investigating hourglass C-3 WPs in phonon spectra and other boson systems, and would also attract widespread interest.

III. MATERIAL CANDIDATE: α-$LiIO_3$

Based on first-principles calculations, we confirm our idea by predicting the existing material α-$LiIO_3$ with SG 173 ($P6_3$) as the first material candidate with (hourglass) C-3 Weyl phonons. α-$LiIO_3$ can be prepared by neutralizing stoichiometric quantities of Li_2CO_3 and HIO_3 in distilled water, i.e., $Li_2CO_3 + 2HIO_3 \rightarrow 2LiIO_3 + H_2O + CO_2$. The solution can be evaporated at 313 K to obtain the α-$LiIO_3$ crystallites [69]. In our calculation, the structure of α-$LiIO_3$ is relaxed, and the optimized crystal structure is shown in Fig. 2(a). The determined lattice constants ($a = b = 5.396$ Å and $c = 5.048$ Å) are in a good agreement with the experimental values [69]. The Li, I, and O atoms of α-$LiIO_3$ locate at $2a$, $2b$, and $6c$ Wyckoff positions, respectively. More details about the computational methods can be found in the SM [61].

According to Table I, SG 173 may exhibit an hourglass C-3 WP on the Γ-A path. In Fig. 3(a), we plot the phonon band structure of α-$LiIO_3$ along high-symmetry paths in the Brillouin zone (BZ), where multiple hourglass-type bands indeed are observed on the Γ-A path, consistent with the above symmetry analysis. Here, we focus on the hourglass-type bands around 20 THz, for which the enlarged plot is shown in Fig. 3(b). The hourglass-type bands are formed by the four phonon branches (Nos. 25–28). Moreover, one observes that these hourglass-type bands are well separated from other bands [see Fig. 3(b)], which would be beneficial for experimental detections.

We then study the neck crossing point of the hourglass in Fig. 3(b), which should be a C-3 WP according to our symmetry analysis. It locates at $\boldsymbol{K} = (0, 0, 0.061)$ in the unit of reciprocal lattice vectors. The $\boldsymbol{k} \cdot \boldsymbol{p}$ effective Hamiltonian of the neck crossing point expanded up to leading order reads [42]

$$\mathcal{H}_{\text{C-3}}(\boldsymbol{q}) = \mathcal{H}_0(\boldsymbol{q}) + \begin{bmatrix} 0 & \alpha_1 q_+^3 + \alpha_2 q_-^3 \\ \alpha_1^* q_-^3 + \alpha_2^* q_+^3 & 0 \end{bmatrix}, \quad (1)$$

with

$$\mathcal{H}_0(\boldsymbol{q}) = \sum_{i=0}^{3} q_z \left(c_{i,1} + c_{i,2} q_z + c_{i,3} q_z^2 + c_{i,4} q^2\right) \sigma_i. \quad (2)$$

Here, the energy and momentum $\boldsymbol{q}$ are measured from the neck crossing point $\boldsymbol{K}$. σ_i $(i = 0, 1, 2, 3)$ is the Pauli matrix, $q_\pm = q_x \pm i q_y$, $q = \sqrt{q_x^2 + q_y^2 + q_z^2}$, and α and c denote complex and real parameters depending on material details, respectively. According to Eq. (1), the band splitting around the neck crossing point is linear along the q_z direction and cubic in the q_x−q_y plane, which is confirmed by our calculations [see Fig. 3(d)]. The inset of Fig. 3(b) also plots the Wilson loop of a sphere enclosing the neck crossing point, and shows its topological charge is $\mathcal{C} = -3$. These results undoubtedly demonstrate that the neck crossing point of the hourglass is a C-3 WP.

Since the α-$LiIO_3$ has $\mathcal{T}$ symmetry, another C-3 WP with $\mathcal{C} = -3$ will appear at the $-\boldsymbol{K}$ point. Due to the

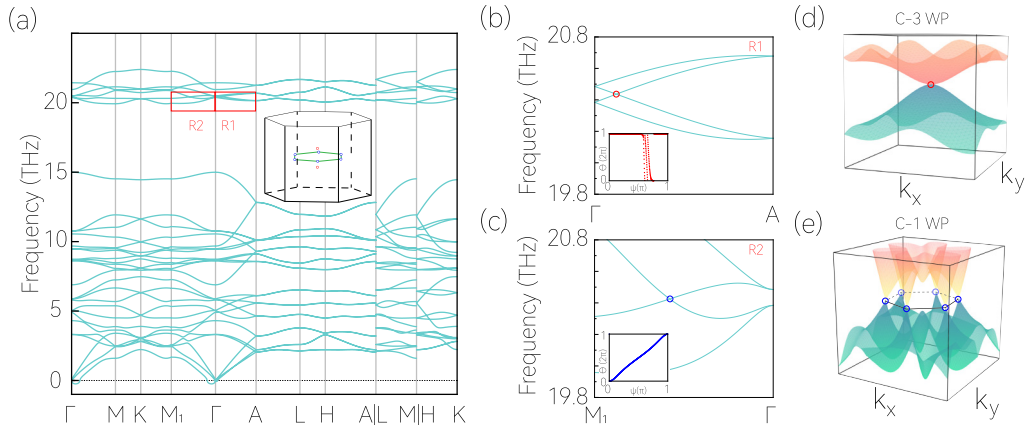

FIG. 3. (a) Calculated phonon spectrum of α-$LiIO_3$ along high-symmetry paths. The inset in (a) shows the positions of the two C-3 WPs and the six C-1 WPs appearing around 20 THz. (b) and (c) respectively show the enlarged phonon dispersions of R1 and R2 regions in (a). The hourglass C-3 WP (conventional C-1 WP) can be clearly observed in (b) [(c)]. The inset in (b) [(c)] shows the obtained Wilson loop of the WP in R1 (R2). (d) plots the cubic dispersion around the hourglass C-3 WP in the plane perpendicular to Γ-A path. (e) presents the 3D plot of the phonon spectrum at $k_z = 0$ plane. The red and blue circles in (a)–(e) show the positions of C-3 and C-1 WPs, respectively.

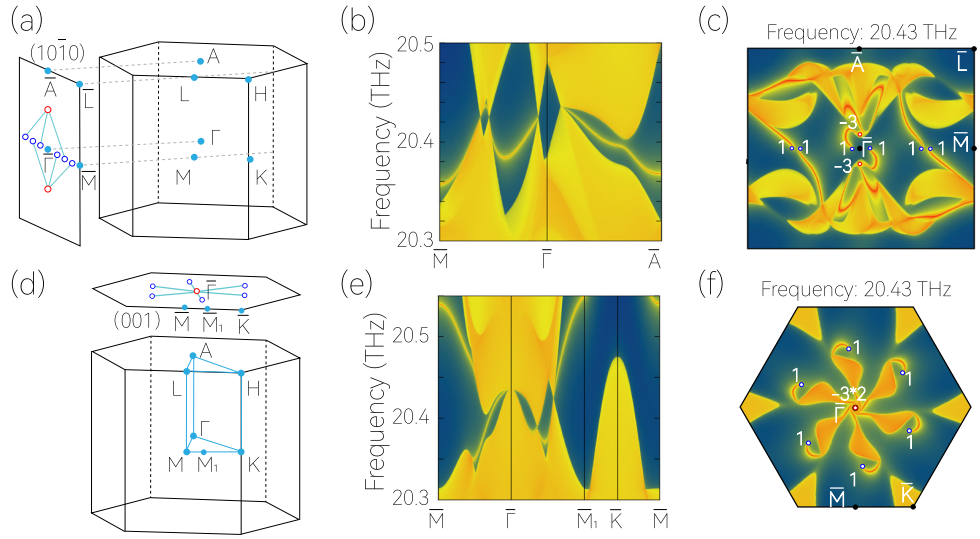

FIG. 4. (a) and (d) show the (10$\bar{1}$0) and (001) surface BZs, along with the schematics of surface modes. The projections of the C-3 and C-1 WPs are marked by red and blue circles, respectively. Projected spectrum on the (b) (10$\bar{1}$0) and (e) (001) surfaces of α-$LiIO_3$. (c) and (f) show the constant energy slices at 20.43 THz for the (10$\bar{1}$0) and (001) surfaces, respectively.

Nielsen-Ninomiya no-go theorem, the net topological charge of the system would be zero. Therefore, there must exist other WPs formed by the phonon branches No. 26 and No. 27. After a careful scanning, we do find six C-1 WPs at the $k_z = 0$ plane, connected by $\tilde{C}_{6z,3}$, as shown in Figs. 3(c) and 3(e). The position for one of the C-1 WPs is $(-0.040, 0.310, 0.000)$, and the topological charge for each of the six C-1 WPs is obtained as $\mathcal{C} = 1$ [see Fig. 3(c)]. Detailed information on the two hourglass C-3 WPs and the six C-1 WPs can be found in the SM [61]. Hence, the two hourglass C-3 WPs and the six C-1 WPs together constitute a Weyl complex, for which the net topological charge vanishes. Notice that the Weyl complex here is different from the triangular Weyl complex proposed by Wang *et al.* in the phonon spectra of α-SiO_2 [55]. There, the Weyl complex is composed of one C-2 WP and two C-1 WPs. Since the six C-1 WPs locate at generic positions of the BZ, they do not have $\mathcal{T}$ and any crystalline symmetry. Then, the Hamiltonian for each of the C-1 WPs reads

$$\mathcal{H}_{\text{C-1}}(\boldsymbol{q}) = \sum_{i=0}^{3} (c_{i,1}q_x + c_{i,2}q_y + c_{i,3}q_z)\sigma_i, \tag{3}$$

with c's the real parameters. Again, the energy and momentum in Eq. (3) are measured from the corresponding C-1 WP.

IV. TRIPLE- AND SEXTUPLE-HELICOID SURFACE ARC STATES

In the following, we come to examine the novel surface states associated with the hourglass C-3 WP in α-$LiIO_3$. We first consider the (10$\bar{1}$0) surface [see Fig. 4(a)]. For this surface, the two bulk hourglass C-3 WPs will be projected into the $\bar{\Gamma}$-$\bar{A}$ path in the surface BZ, while the six bulk C-1 WPs are projected into the $\bar{\Gamma}$-$\bar{M}$ path, as illustrated in Fig. 4(a). Since the two C-3 WPs are projected to different positions in the surface BZ, one can expect that the three surface arc states of each C-3 WP around the projected point on the boundary would form a triple helicoid, similar to the other nodal points with nonzero Chern number [50,70,71]. Besides, because the two C-3 WPs have the same chirality, there in total exist six surface arcs on the (10$\bar{1}$0) surface. These surface arcs emerge from the surface projection of the two C-3 WPs and end at the surface projections of the six C-1 WPs. Due to the presence of $\mathcal{T}$ symmetry, the surface mode may form the pattern in Fig. 4(a). This analysis on the surface mode is confirmed by our calculation results in Figs. 4(b) and 4(c), which respectively show the projected spectrum and the isofrequency surface contour at 20.43 THz of α-$LiIO_3$ on the (10$\bar{1}$0) surface.

In contrast, the surface mode on the (001) surface shows completely different features. The projected spectrum for α-$LiIO_3$ on the (001) surface along the surface paths $\bar{M}$-$\bar{\Gamma}$-$\bar{M}_1$-$\bar{K}$-$\bar{M}$ is plotted in Fig. 4(e), and the isofrequency surface contour at 20.43 THz is shown in Fig. 4(f). For the (001) surface, the two bulk hourglass C-3 WPs are projected to the same position, namely, the $\bar{\Gamma}$ point on the (001) surface BZ. Thus, there must exist six surface arcs connected to the $\bar{\Gamma}$ point, leading to a sextuple helicoid instead of a triple helicoid, as schematically shown in Fig. 4(d). This novel surface mode also is confirmed by our calculation in Fig. 4(f).

V. CONCLUSIONS

In summary, using symmetry analysis, we show that the C-3 WP only appears at the sixfold rotation axis and can be further classified as normal C-3 WP and hourglass C-3 WP. For the former, it can be realized in 12 out of 230 SGs, while the latter only occurs in two SGs. We then predict several realistic materials that host hourglass C-3 Weyl phonons. As a representative material candidate, α-$LiIO_3$ exhibits one pair of C-3 WPs and six C-1 WPs at a certain frequency range in phonon spectra, leading to a novel Weyl complex. Moreover, the triple- and sextuple-helicoid surface arc states can be clearly found in the (10$\bar{1}$0) surface and (001) surface of

α-$LiIO_3$, respectively. Thus, our work uncovers a new type of Weyl phonon, offers a method to search for (hourglass) C-3 Weyl phonons in 230 SGs, and proposes realistic materials to realize the ideal hourglass C-3 Weyl phonons and clean sextuple-helicoid phonon surface states. Furthermore, our results are not limited to phonon spectra but can also be applied to other boson systems, such as photon or magnon systems.

Note added. Recently, we became aware of Ref. [72], which has some overlaps with our work.

ACKNOWLEDGMENTS

The authors thank J. Xun for helpful discussions. This work is supported by the National Natural Science Foundation of China (Grants No. 12004035, No. 12234003, and No. 12061131002), the Natural Science Foundation of Chongqing (Grant No. CSTB2022NSCQ-MSX0283), the National Key R&D Program of China (Grant No. 2020YFA0308800), and the National Natural Science Fund for Excellent Young Scientists Fund Program (Overseas).

[1] X. Wan, A. M. Turner, A. Vishwanath, and S. Y. Savrasov, Phys. Rev. B **83**, 205101 (2011).
[2] N. P. Armitage, E. J. Mele, and A. Vishwanath, Rev. Mod. Phys. **90**, 015001 (2018).
[3] S. Guan, Z.-M. Yu, Y. Liu, G.-B. Liu, L. Dong, Y. Lu, Y. Yao, and S. A. Yang, npj Quantum Mater. **2**, 23 (2017).
[4] H. Weng, C. Fang, Z. Fang, B. A. Bernevig, and X. Dai, Phys. Rev. X **5**, 011029 (2015).
[5] L. X. Yang, Z. K. Liu, Y. Sun, H. Peng, H. F. Yang, T. Zhang, B. Zhou, Y. Zhang, Y. F. Guo, M. Rahn *et al.*, Nat. Phys. **11**, 728 (2015).
[6] S.-M. Huang, S.-Y. Xu, I. Belopolski, C.-C. Lee, G. Chang, B. Wang, N. Alidoust, G. Bian, M. Neupane, C. Zhang *et al.*, Nat. Commun. **6**, 7373 (2015).
[7] A. A. Soluyanov, D. Gresch, Z. Wang, Q.-S. Wu, M. Troyer, X. Dai, and B. A. Bernevig, Nature (London) **527**, 495 (2015).
[8] Y. Sun, S.-C. Wu, M. N. Ali, C. Felser, and B. Yan, Phys. Rev. B **92**, 161107(R) (2015).
[9] J. Ruan, S.-K. Jian, D. Zhang, H. Yao, H. Zhang, S.-C. Zhang, and D. Xing, Phys. Rev. Lett. **116**, 226801 (2016).
[10] G. Autès, D. Gresch, M. Troyer, A. A. Soluyanov, and O. V. Yazyev, Phys. Rev. Lett. **117**, 066402 (2016).
[11] H. Weng, C. Fang, Z. Fang, and X. Dai, Phys. Rev. B **94**, 165201 (2016).
[12] Z. Wang, M. G. Vergniory, S. Kushwaha, M. Hirschberger, E. V. Chulkov, A. Ernst, N. P. Ong, R. J. Cava, and B. A. Bernevig, Phys. Rev. Lett. **117**, 236401 (2016).
[13] W. Shi, L. Muechler, K. Manna, Y. Zhang, K. Koepernik, R. Car, J. van den Brink, C. Felser, and Y. Sun, Phys. Rev. B **97**, 060406(R) (2018).
[14] Q. Xu, E. Liu, W. Shi, L. Muechler, J. Gayles, C. Felser, and Y. Sun, Phys. Rev. B **97**, 235416 (2018).
[15] G. Chang, S.-Y. Xu, D. S. Sanchez, S.-M. Huang, C.-C. Lee, T.-R. Chang, G. Bian, H. Zheng, I. Belopolski, N. Alidoust *et al.*, Sci. Adv. **2**, e1600295 (2016).
[16] K. Koepernik, D. Kasinathan, D. V. Efremov, S. Khim, S. Borisenko, B. Büchner, and J. van den Brink, Phys. Rev. B **93**, 201101(R) (2016).
[17] B. Lv, N. Xu, H. Weng, J. Ma, P. Richard, X. Huang, L. Zhao, G. Chen, C. Matt, F. Bisti *et al.*, Nat. Phys. **11**, 724 (2015).
[18] B. Q. Lv, H. M. Weng, B. B. Fu, X. P. Wang, H. Miao, J. Ma, P. Richard, X. C. Huang, L. X. Zhao, G. F. Chen, Z. Fang, X. Dai, T. Qian, and H. Ding, Phys. Rev. X **5**, 031013 (2015).
[19] S. Y. Xu, I. Belopolski, N. Alidoust, M. Neupane, G. Bian, C. Zhang, R. Sankar, G. Chang, Z. Yuan, C. C. Lee, S. M. Huang, H. Zheng, J. Ma, D. S. Sanchez, B. Wang, A. Bansil, F. Chou, P. P. Shibayev, H. Lin, S. Jia, and M. Z. Hasan, Science **349**, 613 (2015).
[20] K. Deng, G. Wan, P. Deng, K. Zhang, S. Ding, E. Wang, M. Yan, H. Huang, H. Zhang, Z. Xu *et al.*, Nat. Phys. **12**, 1105 (2016).
[21] Y. Wu, D. Mou, N. H. Jo, K. Sun, L. Huang, S. L. Bud'ko, P. C. Canfield, and A. Kaminski, Phys. Rev. B **94**, 121113(R) (2016).
[22] C. Bradley and A. Cracknell, *The Mathematical Theory of Symmetry in Solids: Representation Theory for Point Groups and Space Groups* (Oxford University Press, Oxford, England, 2010).
[23] C. Fang, M. J. Gilbert, X. Dai, and B. A. Bernevig, Phys. Rev. Lett. **108**, 266802 (2012).
[24] G. Chang, S.-Y. Xu, H. Zheng, B. Singh, C.-H. Hsu, G. Bian, N. Alidoust, I. Belopolski, D. S. Sanchez, S. Zhang, H. Lin, and M. Z. Hasan, Sci. Rep. **6**, 38839 (2016).
[25] S.-M. Huang, S.-Y. Xu, I. Belopolski, C.-C. Lee, G. Chang, T.-R. Chang, B. Wang, N. Alidoust, G. Bian, M. Neupane *et al.*, Proc. Natl. Acad. Sci. USA **113**, 1180 (2016).
[26] J. Li, Q. Xie, S. Ullah, R. Li, H. Ma, D. Li, Y. Li, and X.-Q. Chen, Phys. Rev. B **97**, 054305 (2018).
[27] L. Jin, X. Zhang, Y. Liu, X. Dai, L. Wang, and G. Liu, Phys. Rev. B **102**, 195104 (2020).
[28] H. He, C. Qiu, X. Cai, M. Xiao, M. Ke, F. Zhang, and Z. Liu, Nat. Commun. **11**, 1820 (2020).
[29] S. Nandy, C. Zeng, and S. Tewari, Phys. Rev. B **104**, 205124 (2021).
[30] D. Chowdhury, A. Banerjee, and A. Narayan, Phys. Rev. B **105**, 075133 (2022).
[31] P. C. Sreeparvathy, C. Mondal, C. K. Barman, and A. Alam, Phys. Rev. B **106**, 085102 (2022).
[32] D. T. Son and B. Z. Spivak, Phys. Rev. B **88**, 104412 (2013).
[33] Q. Chen and G. A. Fiete, Phys. Rev. B **93**, 155125 (2016).
[34] S. Ahn, E. J. Mele, and H. Min, Phys. Rev. B **95**, 161112(R) (2017).
[35] J. Cano, B. Bradlyn, Z. Wang, M. Hirschberger, N. P. Ong, and B. A. Bernevig, Phys. Rev. B **95**, 161306(R) (2017).
[36] R. M. A. Dantas, F. Peña Benitez, B. Roy, and P. Surówka, Phys. Rev. Res. **2**, 013007 (2020).
[37] B.-J. Yang and N. Nagaosa, Nat. Commun. **5**, 4898 (2014).
[38] B.-J. Yang, T. Morimoto, and A. Furusaki, Phys. Rev. B **92**, 165120 (2015).
[39] Z. Gao, M. Hua, H. Zhang, and X. Zhang, Phys. Rev. B **93**, 205109 (2016).
[40] Z.-M. Yu, W. Wu, X.-L. Sheng, Y. X. Zhao, and S. A. Yang, Phys. Rev. B **99**, 121106(R) (2019).

[41] W. Wu, Z.-M. Yu, X. Zhou, Y. X. Zhao, and S. A. Yang, Phys. Rev. B **101**, 205134 (2020).
[42] Z.-M. Yu, Z. Zhang, G.-B. Liu, W. Wu, X.-P. L. Li, R.-W. Zhang, S. A. Yang, and Y. Y., Sci. Bull. **67**, 375 (2022).
[43] T. Zhang, R. Takahashi, C. Fang, and S. Murakami, Phys. Rev. B **102**, 125148 (2020).
[44] Q.-B. Liu, Y. Qian, H.-H. Fu, and Z. Wang, npj Comput. Mater. **6**, 95 (2020).
[45] Q.-B. Liu, Z. Wang, and H.-H. Fu, Phys. Rev. B **103**, L161303 (2021).
[46] Z. Zhang, G.-B. Liu, Z.-M. Yu, S. A. Yang, and Y. Yao, Phys. Rev. B **105**, 104426 (2022).
[47] G. Xu, H. Weng, Z. Wang, X. Dai, and Z. Fang, Phys. Rev. Lett. **107**, 186806 (2011).
[48] D. Bulmash, C.-X. Liu, and X.-L. Qi, Phys. Rev. B **89**, 081106(R) (2014).
[49] H. Miao, T. T. Zhang, L. Wang, D. Meyers, A. H. Said, Y. L. Wang, Y. G. Shi, H. M. Weng, Z. Fang, and M. P. M. Dean, Phys. Rev. Lett. **121**, 035302 (2018).
[50] T. Zhang, Z. Song, A. Alexandradinata, H. Weng, C. Fang, L. Lu, and Z. Fang, Phys. Rev. Lett. **120**, 016401 (2018).
[51] B. W. Xia, R. Wang, Z. J. Chen, Y. J. Zhao, and H. Xu, Phys. Rev. Lett. **123**, 065501 (2019).
[52] J.-Y. You, X.-L. Sheng, and G. Su, Phys. Rev. B **103**, 165143 (2021).
[53] Y. J. Jin, Z. J. Chen, X. L. Xiao, and H. Xu, Phys. Rev. B **103**, 104101 (2021).
[54] J. Li, J. Liu, S. A. Baronett, M. Liu, L. Wang, R. Li, Y. Chen, D. Li, Q. Zhu, and X.-Q. Chen, Nat. Commun. **12**, 1204 (2021).
[55] R. Wang, B. W. Xia, Z. J. Chen, B. B. Zheng, Y. J. Zhao, and H. Xu, Phys. Rev. Lett. **124**, 105303 (2020).
[56] Y. Liu, N. Zou, S. Zhao, X. Chen, Y. Xu, and W. Duan, Nano Lett. **22**, 2120 (2022).
[57] N. Li, J. Ren, L. Wang, G. Zhang, P. Hänggi, and B. Li, Rev. Mod. Phys. **84**, 1045 (2012).
[58] Y. Liu, X. Chen, and Y. Xu, Adv. Funct. Mater. **30**, 1904784 (2020).
[59] S. Singh, Q. S. Wu, C. Yue, A. H. Romero, and A. A. Soluyanov, Phys. Rev. Mater. **2**, 114204 (2018).
[60] X.-Q. Chen, J. Liu, and J. Li, The Innovation **2**, 100134 (2021).
[61] See Supplemental Material at http://link.aps.org/supplemental/10.1103/PhysRevB.106.214309 for more material candidates with hourglass C-3 WP and computational methods, which includes Refs. [73–77].
[62] X. Wang, F. Zhou, Z. Zhang, W. Wu, Z.-M. Yu, and S. A. Yang, Phys. Rev. B **106**, 195129 (2022).
[63] Z. Wang, A. Alexandradinata, R. J. Cava, and B. A. Bernevig, Nature (London) **532**, 189 (2016).
[64] S. M. Young and C. L. Kane, Phys. Rev. Lett. **115**, 126803 (2015).
[65] T. Bzdušek, Q. Wu, A. Rüegg, M. Sigrist, and A. A. Soluyanov, Nature (London) **538**, 75 (2016).
[66] S.-S. Wang, Y. Liu, Z.-M. Yu, X.-L. Sheng, and S. A. Yang, Nat. Commun. **8**, 1844 (2017).
[67] S. Li, Y. Liu, S.-S. Wang, Z.-M. Yu, S. Guan, X.-L. Sheng, Y. Yao, and S. A. Yang, Phys. Rev. B **97**, 045131 (2018).
[68] W. Wu, Y. Jiao, S. Li, X.-L. Sheng, Z.-M. Yu, and S. A. Yang, Phys. Rev. Mater. **3**, 054203 (2019).
[69] J. De Boer, F. Van Bolhuis, and R. V. Olthof-Hazekamp, Acta Crystallogr. **21**, 841 (1966).
[70] C. Fang, L. Lu, J. Liu, and L. Fu, Nat. Phys. **12**, 936 (2016).
[71] C. Cui, X.-P. Li, D.-S. Ma, Z.-M. Yu, and Y. Yao, Phys. Rev. B **104**, 075115 (2021).
[72] G. Liu, Z. Chen, P. Wu, and H. Xu, Phys. Rev. B **106**, 214308 (2022).
[73] G. Kresse and J. Furthmüller, Phys. Rev. B **54**, 11169 (1996).
[74] J. P. Perdew, K. Burke, and M. Ernzerhof, Phys. Rev. Lett. **77**, 3865 (1996).
[75] P. E. Blöchl, Phys. Rev. B **50**, 17953 (1994).
[76] A. Togo and I. Tanaka, Scr. Mater. **108**, 1 (2015).
[77] Q. Wu, S. Zhang, H.-F. Song, M. Troyer, and A. A. Soluyanov, Comput. Phys. Commun. **224**, 405 (2018).